PHYSICAL REVIEW C VOLUME 23, NUMBER 6 JUNE 1981

Influence of complex states and deformation on neutron pairing vibrations in the even Sm isotopes

G. L. Struble, L. G. Mann, R. G. Lanier, and W. M. Buckley
Lawrence Livermore Laboratory, University of California, Livermore, California 94550

J. Kern
Lawrence Livermore Laboratory, University of California, Livermore, California 94550 and University of Fribourg, Fribourg, Switzerland

G. Crawley and S. Gales*
Michigan State University, East Lansing, Michigan 48824

D. Mueller and F. Girshick
Princeton University, Princeton, New Jersey 08540

(Received 3 October 1980)

The (p,t) reaction has been used to study the behavior of two-neutron holes in the even Sm isotopes at high excitation energy. The tritons were analyzed with a counter telescope, quadrupole-dipole-dipole-dipole spectrograph, and an Enge split-pole spectrograph. Both broad and narrow structures are observed at excitation energies above 5 MeV. Some of these can be interpreted in terms of the low-energy structure of ^{142}Sm.

[NUCLEAR REACTIONS ^{144,148,150,152,154}Sm(p,t), E_p=42 MeV; enriched targets, QDDD, Enge split-pole spectrograph. Measured $\sigma(E_t, \theta_t)$. Deduced ^{142}Sm levels E, J; relate ^{142}Sm levels to high-energy structure in heavier Sm isotopes.]

I. INTRODUCTION

The damping of simple structures at high excitation energies because of the large density of neighboring complex states is a fundamental line broadening problem in quantum mechanics. The best-studied example from nuclear physics is the giant dipole resonance.[1] These 1^- states are isovector particle-hole (p-h) excitations which, in the Sm region, occur at ~15 MeV in excitation energy. Phenomenologically, they are described as a vibration where the normal coordinate is the distance between the center of mass of the neutrons and the protons. More recently, other giant (p-h) vibrations have been discovered, including the isoscalar monopole[2] and the isoscalar and isovector quadrupole modes.[1] There are, of course, other structures which occur at a large excitation energy including analogue states and single-particle states.[1]

In 1977 Broglia and Bes[3] predicted the existence of high-lying pairing resonances. Shortly thereafter, Crawley *et al.*[4] reported enhanced two-hole strength at 8 MeV in the Sn isotopes excited by the (p,t) reaction. Such intense, high-energy, particle-particle (p-p) or hole-hole (h-h) modes depend on the existence of a large shell gap which separates them from other states with the same spin and parity. Thus, such modes are not expected in deformed nuclei.

The Sm isotopes are very interesting for testing these ideas since there are five stable even-even isotopes in the region from $N=82$ to 92. In this one sequence of isotopes, it is possible to study the underlying two-hole structure, i.e., the low-energy excitations of ^{142}Sm, and observe its behavior at higher excitation energy in spherical, transitional, and deformed nuclei. Furthermore, since one has a measure of the spectroscopic strength of the individual two-hole excitations, one can quantitatively determine how much of the strength in any resonant structure is due to states that involve nucleons in the valence shell.

We published the preliminary results of this investigation in a recent Letter.[5] In the present paper we present all of our experimental results, give a detailed discussion of the level structure of ^{142}Sm, and argue that remnants of this structure remain at energies above 4 MeV in those heavier Sm isotopes which we have studied.

In Sec. II we will discuss a series of (p,t) experiments conducted at Princeton University and at Michigan State University (MSU) to associate the low-energy states of ^{142}Sm with structures at ~6 MeV excitation in ^{146}Sm, ^{148}Sm, ^{150}Sm, and ^{152}Sm. In Sec. III we will present the experimental data.

Section IV is a discussion and interpretation of the results, while Sec. V contains a summary and conclusion.

II. EXPERIMENTAL PROCEDURES

Each of the stable even-mass Sm isotopes was studied by means of the (p,t) reaction with 42-MeV protons. Experiments were performed at both the Princeton University and the MSU cyclotron facilities. At Princeton a solid-state, silicon, three-crystal telescope was used with metal foil targets ~3 mg/cm^2 to survey the energy region from 0 to ~20-MeV excitation in each residual nucleus. The telescope consisted of a ΔE detector 300 μm thick operated in coincidence with a second detector 3.3 mm thick which stopped all the tritons. The third detector was operated in anticoincidence to reject events due to protons and deuterons. The rate of data accumulation for tritons from the (p,t) reaction was severely limited ($\lesssim$2 Hz) because of the need to restrict the total counting rate, which was dominated by the elastically scattered protons, to an acceptable upper limit of 20 kHz.

In spite of the problems caused by high proton fluxes in the detector, the triton data clearly showed gross features which consisted of a broad resonance and narrow structures at several MeV of excitation energy. The quadrupole-dipole-dipole-dipole (QDDD) spectrograph[6] at Princeton was used with a thin (~100 μg/cm^2) target of ^{148}Sm in order to examine the narrow structures with high resolution. The spectrograph covered an energy range of 2.4 MeV and had a resolution of 15 keV full width at half maximum (FWHM) in these experiments. Energy calibration in the region of 4.8-MeV excitation in ^{146}Sm was determined with an accuracy of ±25 keV by using (p,t) data from the same ^{148}Sm target. This calibration was based on the known states up to 3.138 MeV in ^{146}Sm populated by the (p,t) reaction and on an extrapolation in the magnetic field to the 4.8-MeV region of excitation.

In order to eliminate the problem of protons in the detector and still examine a wide range of excitation energies in a reasonable amount of accelerator time, a series of experiments were performed at MSU using the Enge split-pole spectrograph. Table I gives pertinent data on the targets. All targets were metal foils except the ^{144}Sm, which was evaporated onto a thin carbon backing. In general, the target thicknesses represent a compromise between the desires for optimum energy resolution and for high data-accumulation rates. High counting rates were needed because of the large number of runs required for complete angular distribution data on all five targets. On the other hand, good energy resolution was especially important with the ^{144}Sm target because of the need to resolve the low-lying discrete states in ^{142}Sm. Under the conditions of our experiments, resolution with the ^{144}Sm target was 35 keV FWHM.

TABLE I. Sm targets used with the Enge split-pole spectrograph.

	Thickness (mg/cm^2)	Enrichment (%)	(p,t) Q value[a] (MeV)
^{144}Sm	0.44	96.5	−10.647
^{148}Sm	2.2	96.5	−6.012
^{150}Sm	2.3	95.5	−5.375
^{152}Sm	3.2	91.3	−5.373
^{154}Sm	3.0	98.6	−5.354

[a] Reference 7.

Tritons were detected in a 50-cm-long delay-line gas counter[7] backed by a plastic scintillator. The range of energies detected was 15 MeV and the spectrograph solid angle was 1.22 msr. The incident proton energy was 42 MeV to conform to the Princeton experiments. At this energy the maximum stable field of the Enge spectrograph was insufficient to focus tritons from the ground-state transitions onto the detector, except for the ^{144}Sm target.

Since the ground-state peaks were generally not available for energy calibration, the MSU data were calibrated with information obtained from the counter telescope. A linear energy calibration for the counter telescope was based on the ground state Q values of the Sm(p,t) reaction (Table I).[8] This calibration established the energy of the most prominent narrow peak in each target within an uncertainty of ±100 keV. The ^{16}O$(p,t)^{14}$O ground-state transition (Q value = −20.406 MeV), which appeared prominently with each target, was also used as a calibration point for the MSU data.

Absolute cross sections from the MSU data were based on a comparison of elastically scattered proton data at 15°, 18°, and 21° in the Enge spectrograph with elastic scattering cross sections calculated with the optical model. The beam current was monitored by counting elastically scattered protons in a NaI detector at 90° and also by a beam current integrator at the Faraday cup. The error in absolute cross sections due to this normalization procedure depends primarily on the validity of the optical model calculation, which we estimate is within ±10%.

III. RESULTS

Figure 1 shows the triton spectrum obtained with the Enge split-pole spectrometer at 20° for

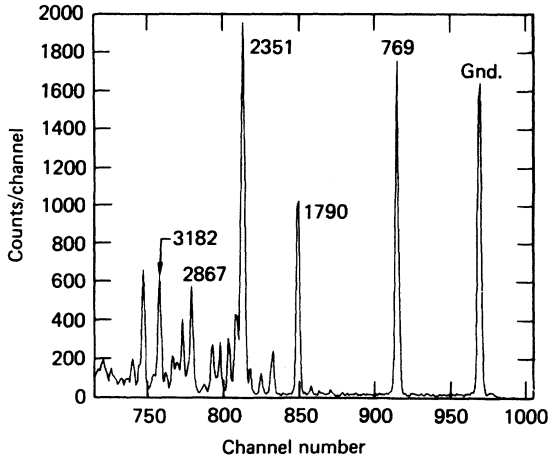

FIG. 1. Triton spectrum obtained with the Enge split-pole spectrograph at 20° for the $^{144}Sm(p,t)^{142}Sm$ reaction. The portion of the spectrum up to excitation energies of 3800 keV is shown. Some prominent lines are labeled in keV.

states up to ~3.7 MeV populated by the $^{144}Sm(p,t)$ reaction. The 35-keV resolution in this experiment is sufficient to resolve most of the states below 2 MeV.

The spectrum at each angle was analyzed by using the interactive spectral analysis program FITEK.[9] Table II lists the excitation energies and cross sections for those states which we have observed below 3.25 MeV. The errors are purely statistical with no estimate made for any systematic effects. Also shown in Table II are the L values suggested by the angular distribution data for two-neutron transfer and the level energies and spin-parities determined by previous work.[10-12]

Figures 2 and 3 show the triton angular distributions associated with states in ^{142}Sm. We have grouped together states which show (or in the case of Fig. 3 fail to show) similar diffraction patterns. In the three panels of Fig. 2 we also present the results of a distorted-wave Born approximation (DWBA) calculation for $L=0$, 2, and 4, respectively.[13] The parameters used in the calculation are given in Table III. The parameters are taken from the compilation of Perey and Perey[14] with the exception that the radius for the real part of the triton optical potential has been increased thirty percent in order to move the peaks of the diffraction pattern to a more forward angle, giving better agreement with the ground-state $L=0$ data. The value of these data and DWBA calculations for assigning spins and parities will be discussed in the following section.

Figure 4 shows the data up to ~15-MeV excitation obtained at 20° from the beam with the Enge split-pole spectrograph for all the Sm targets.

TABLE II. Summary of levels in ^{142}Sm.

$^{144}Sm(p,t)^{142}Sm$ (this work)				Decay data[a]	
Channel	E_x (keV)[b]	L	$\sigma(5°-58°)$[b,c] (μb)	E_x (keV)	J^π
969.5	0	0	105 (5)	0	0^+
915.0	769(1)	2	137 (6)	768.0	2^+
871.3	1453(4)	(0?)	5.2 (6)	(1450.2)[d]	(0^+)[d]
863.6	1572(6)				
858.0	1659(3)	(2?)	3.5 (7)	1657.6	(2^+)
				1784.1	3^-
849.5	1790(1)	4	69 (3)	1791.3	4^+
832.5	2052(1)	2	20 (2)	2055.5	2^+
824.9	2168(1)	0	5.9 (7)		
817.6	2280(3)	0	8.1(12)		
812.9	2351(1)		172 (7)	2347.9	5^-
				2372.0	7^-
808.5	2418(2)	(4)	39 (3)	2420.0	(6^+)
803.3	2497(2)		18 (2)		
797.7	2582(2)	4	17 (2)		
792.8	2656(2)		20 (2)		
786.8	2747(6)	(2)	5.0(12)		
778.8	2867(1)	4	32 (3)		
				2912.0	
773.0	2955(2)	4	20 (2)		
769.5	3007(5)		13 (2)		
766.5	3052(3)		15 (2)		
762.1	3118(4)		6.7(10)	3113	
757.8	3182(1)		40 (3)		
				3220	
753.6	3245(4)		8.2(14)		

[a] Reference 9.

[b] Statistical errors in the least significant digits are given in parentheses.

[c] Cross section for tritons emitted within the solid angle between 5° and 58° with the beam axis.

[d] See discussion, Ref. 9 (p. 559).

The ground-state transition (at $Q=-10.647$ MeV) is seen only for the ^{144}Sm target. Each spectrum has been expanded or contracted by a few percent and shifted along the abscissa as needed in order to present all the data on a common Q-value scale. The Q-value scale is slightly nonlinear because of the spectrometer characteristics.

A localization of two-neutron transfer strength appears in the ^{148}Sm and ^{150}Sm targets as a broad resonance "bump" several MeV wide and centered at an excitation energy near 6 MeV. The Q value of the bumps corresponds to the region of discrete peaks in ^{142}Sm. Several much narrower structures are prominent among the heavier targets at excitation energies $\gtrsim 4$ MeV. The correlations between these structures and the low-lying states in ^{142}Sm will be discussed. The peaks labeled e in Fig. 4 were also prominent in the counter telescope data.

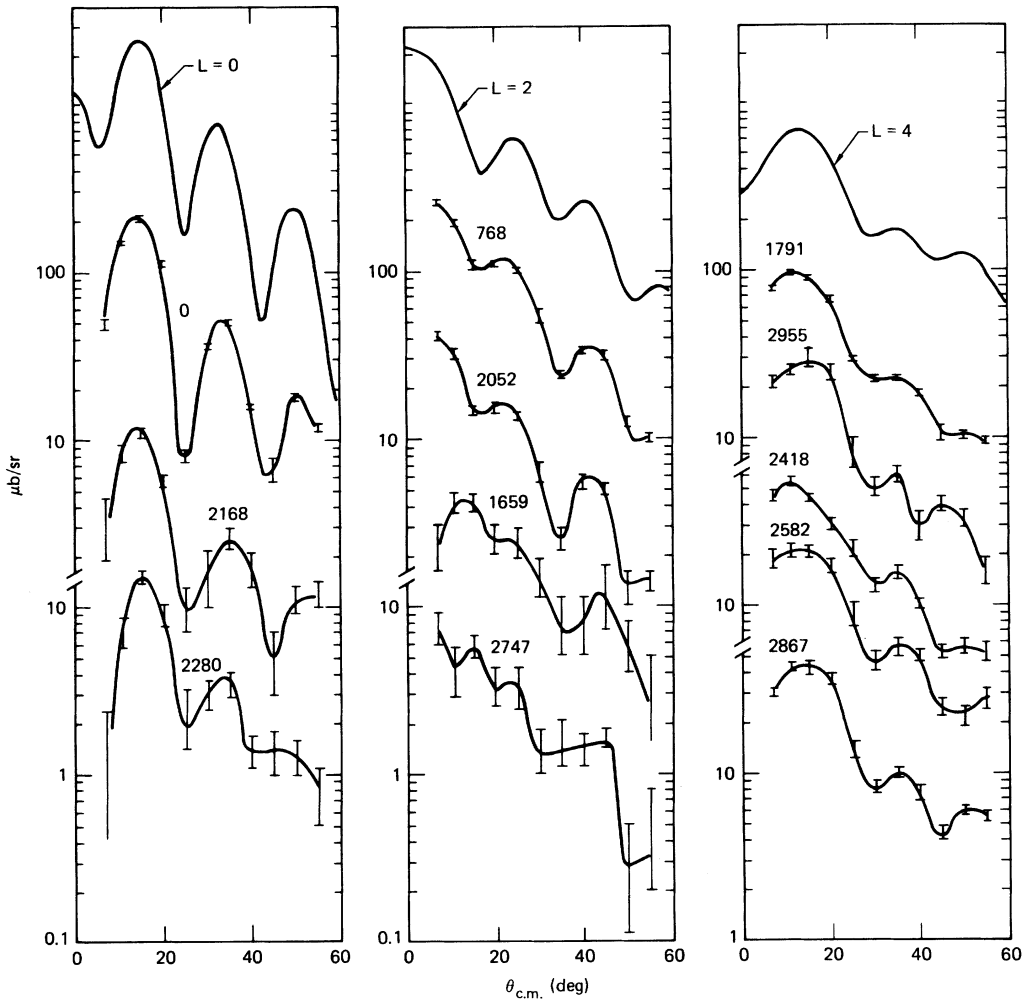

FIG. 2. Triton angular distributions for the ^{144}Sm$(p,t)^{142}$Sm reaction. The top curves are the results of DWBA calculations. The lines through the points are only to guide the eye. Energies of the states are given in keV.

We compared cross sections and angular distributions for the region of the broad resonance by summing the counts within a fixed Q-value window. The window extended from $Q=-16.5$ to -8.8 MeV, an arbitrary choice which we judged to bracket the bump in the ^{148}Sm and ^{150}Sm targets. We chose a second, narrower window immediately above the excitation energy of the bump window, extending from $Q=-19.1$ to -16.5 MeV, in order to examine the behavior at higher excitation energies. These integration regions are indicated in Fig. 4. Figures 5 and 6 show the angular distributions observed in the two windows. In Fig. 6 the ^{150}Sm data have been shifted upwards for clarity by a factor of 1.35. The structureless behavior of these angular distributions is not surprising since we expect many states with different spins to contribute.

Figure 7 shows a spectrum obtained with the QDDD spectrograph at Princeton for the thin ^{148}Sm target in the region of the narrow peak labeled *c* in Fig. 4. We expect a large density of levels at this excitation energy, of the order of 1.4/keV at 5 MeV.[15] Therefore, in view of our 15-keV FWHM resolution limit, it is not clear that the structure evident in Fig. 7 can be broken down reliably into its individual peak components. The angular distributions of the peaks showed structure which varied from peak to peak but which could not be characterized by unique L values. Since the continuum underlying the peak structure is presumably made up of many unresolved lines this behavior of the angular distributions is not surprising. In the next section we will examine in more detail the peak labeled *S* in Fig. 7. This peak might be expected to show a more definitive angular distribution because of its greater intensity relative to the continuum.

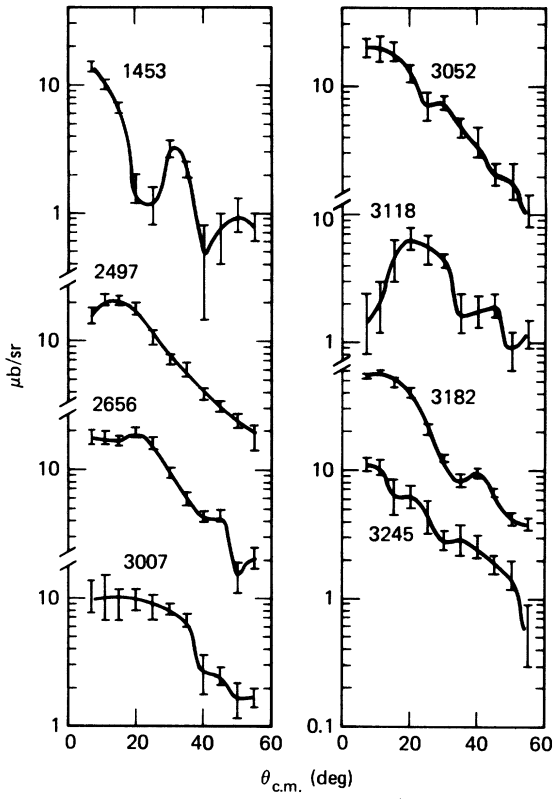

FIG. 3. Triton angular distributions for the ^{144}Sm$(p,t)^{142}$Sm reaction, for states which do not correlate well with any of the DWBA calculated distributions. The 1453-keV level might be $L=0$ (see text).

IV. DISCUSSION

The even-even Sm nuclides offer a particularly interesting series of isotopes for studying high-energy pairing phenomena. The series begins with a single closed shell ($N=82$) at ^{144}Sm and extends to the well-deformed nucleus ^{154}Sm. It is believed[16] that an abrupt shape change occurs between $N=88$ and $N=90$. Thus, ^{150}Sm is spherical and ^{152}Sm is deformed.

If the $N=82$ shell gap is preserved in the series of Sm isotopes, then the two-hole strength associated with single-particle levels below $N=82$ will not be shifted in first order by mixing with the valence orbitals through the residual interactions. Thus, this strength may be sufficiently localized that it will be observed as a giant resonance at a large excitation energy.

However, when the nucleus deforms, the shell structure undergoes drastic changes. A cursory examination of the Nilsson shell-model diagram shows that for $\beta=0.3$, there is no remnant of the $N=82$ gap. Thus, one expects that any strength associated with that gap in the spherical isotopes will be distributed over states in other regions of the spectrum for the deformed nuclei.

In order to recognize and characterize any resonance, it is important to understand the two-hole character of the states in ^{142}Sm. This is best done with the (p,t) reaction.

A. States in ^{142}Sm

The states in ^{142}Sm which contribute strongly to the ^{144}Sm(p,t) strength will be two-neutron hole states in the 82-neutron closed shell. The important single-particle orbitals will be those associated with the low-lying single-neutron hole states in ^{143}Sm. These orbitals are, in the order of their increasing excitations in ^{143}Sm, $2d_{3/2}$, $3s_{1/2}$, $1h_{11/2}$, $2d_{5/2}$, and $1g_{7/2}$.[18] The $3s_{1/2}$ orbital is only 108 keV above the $2d_{3/2}$ ground state, while the $1h_{11/2}$, $2d_{5/2}$, and $1g_{7/2}$ orbitals are at 754, 1107, and 1369 keV of excitation, respectively. However, the $1h_{11/2}$ orbital has a large diagonal pairing energy ($\langle V\rangle_{0^+}\sim 2j+1$) which will lower the energy of the $h_{11/2}^{-2}$ configuration relative to the other two-neutron hole states in ^{142}Sm. Therefore, in the following we will discuss the ^{142}Sm spectrum mainly in terms of the $2d_{3/2}$, $3s_{1/2}$, and $1h_{11/2}$ orbitals.

Before this study, only ten states had been observed below 3 MeV in ^{142}Sm.[17] All of these were disclosed by the decay of high- and low-spin isomers of ^{142}Eu.[10] An in-beam gamma measurement[11] and an earlier (p,t) study[12] yielded less complete results which are consistent with the decay experiments.

1. 0^+ states

Two-hole configurations in the 82-neutron closed shell will account for all of the low-energy (p,t) 0^+ strength. The ground state is presumably a coherent sum of special configurations, each consisting of two holes coupled to angular momentum zero in a particular orbital.

TABLE III. Parameters of the optical potential used for DWBA calculations.

Particle	V (MeV)	R (fm)	a (fm)	W (MeV)	W_D (MeV)	$\bar{R}$ (fm)	$\bar{a}$ (fm)	V_{so} (MeV)	R (fm)	a_{so} (fm)	R_C (fm)
p	−48.62	1.30	0.75	−6.54	11.87	1.32	0.51	−24.8	1.01	0.75	1.30
T	−160.00	1.20	0.72	−22.00	0.0	1.40	0.84	−10.0	1.20	0.72	1.30

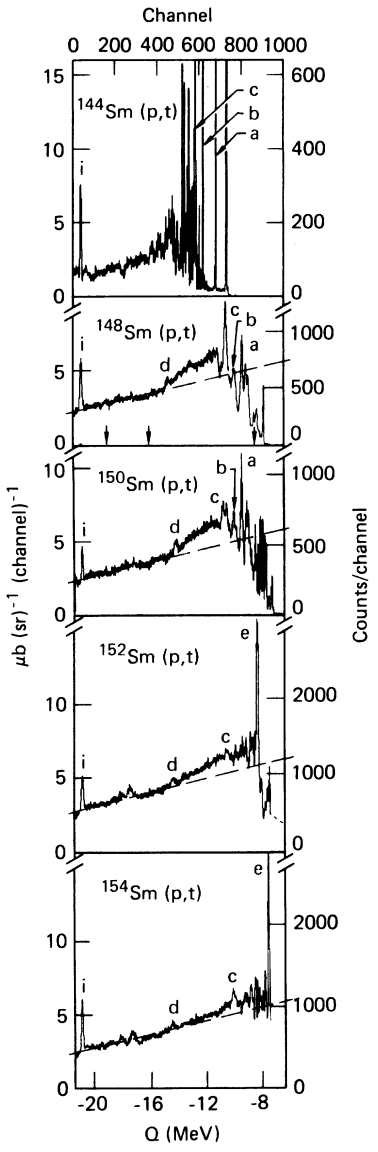

FIG. 4. Triton spectra obtained with the Enge split-pole spectrograph at 20°, displayed on a commom Q-value scale. The energy resolution varies from 35 keV FWHM for the ^{144}Sm target to $\lesssim$60 keV FWHM for the other targets. Peaks *a*, *b*, and *c* in the top panel are from the levels at 769, 1790, and 2351 keV in ^{142}Sm and are shown in detail in Fig. 1. The structure at *d* is of instrumental origin, caused by the joining of two delay lines at the center of the detector. Peak *i* at $Q = -20.406$ MeV is due to oxygen impurity. The three arrows on the abscissa of the ^{148}Sm panel define the integration windows discussed in the text.

We observe an intense state with a Q value close to that predicted for the ground state transition by the Wapstra mass table.[8] It has a clearly defined $L = 0$ angular distribution and on this basis we assign it as the 0^+ ground state.

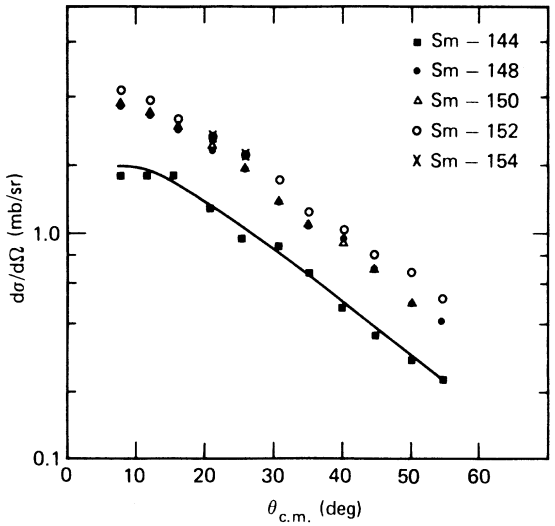

FIG. 5. Angular distributions of the integrated (p,t) strength in the region between $Q = -8.8$ and -16.5 MeV.

There are no other known 0^+ states in ^{142}Sm. However, one expects two additional low-lying 0^+ states since there are three configurations which can be populated with significant two-nucleon pick-up strength. It is well known[1] that the monopole-pairing force mixes 0^+ configurations such that the lowest energy state is coherent with respect to the two-nucleon transfer operator. Thus, almost all of the low-energy, 0^+, two-nucleon transfer strength is associated with the ground state. The other 0^+ states will be only weakly populated.

We have evidence for three additional 0^+ states. The first is the state at 1453 keV, which has 5.0% of the ground-state strength. Its angular distribution (Fig. 3) is not conclusive since the 7° and 11° data are much too high to be compatible with the one-step DWBA predictions for $L = 0$. Nevertheless, the diffraction pattern at backward angles

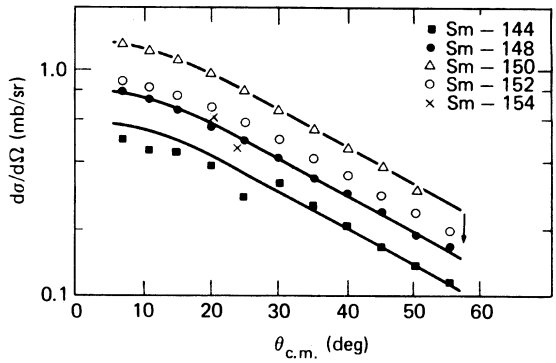

FIG. 6. Same as Fig. 5, but for the region between $Q = -16.5$ and -19.1 MeV. The data for the ^{150}Sm target have been shifted upward by the length of the arrow for clarity.

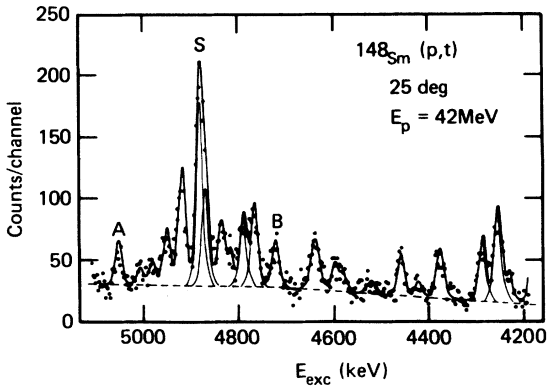

FIG. 7. A high-resolution (15 keV FWHM) triton spectrum obtained with the QDDD spectrograph at 25° for the region around peak *c* in Fig. 4. The solid lines are the result of fitting a standard peak shape to the data. Peak *c* in Fig. 4 corresponds approximately to the group of peaks between *A* and *B*.

certainly resembles that predicted for $L=0$. Moreover, the $N=80$ isotones show systematic evidence for a 0^+ state near 1.5 MeV.[17] As noted by Kennedy *et al.*,[10] such a state at 1450.2 keV in ^{142}Sm could account for an unassigned γ ray of 682.2 keV seen in the decay of ^{142}Eu[g]. Since the character of an $L=0$ angular distribution is associated with the form factor at the nuclear surface, it is not completely surprising that the ground state and first excited 0^+ states, which possess markedly different wave functions, would have somewhat different angular distributions.

The remaining 0^+ states suggested by the angular distribution data occur at 2168 and 2280 keV. They have 5.6% and 7.7% of the ground state strength, respectively.

The existence of four 0^+ states cannot be explained in terms of only three orbitals. Perhaps the $2d_{5/2}$ or $1g_{7/2}$ orbitals, in addition to the $2d_{3/2}$, $3s_{1/2}$, and $1h_{11/2}$ orbitals, are important for 0^+ states in the 2-MeV excitation region. However, proton states in the ^{144}Sm core can also account for additional 0^+ states. There is a 0^+ state at an excitation of 2479 keV in ^{144}Sm.[17] This state is associated with the protons, since the lowest excited 0^+ state for neutrons at the $N=82$ closed shell is the neutron pairing vibration which, according to $N=82$ systematics, should be at $E_{ex}>3$ MeV.[17] Our data suggest that in ^{142}Sm this proton core state (which has no two-neutron pick-up strength) mixes with the third two-neutron-hole state, fragmenting the (p,t) strength between two states.

2. 2^+ excited states

Low-lying 2^+ strength is expected from three configurations: $(2d_{3/2}^{-2})$, $(2d_{3/2}^{-1}3s_{1/2}^{-1})$, and $(1h_{11/2}^{-2})$. Mixing with proton states of the ^{144}Sm core can produce (p,t) strength to additional 2^+ states. We have observed four 2^+ states, three of which were seen in the decay of ^{142}Eu.[10] As in the case of the 0^+ excitations, most of the strength is in the lowest excited state. The second 2^+ state, at 1659 keV, contains only 2.5% of the first excited state's strength and has an anomalous angular distribution. The first excited state in ^{144}Sm is at 1660 keV of excitation and has a spin and parity of 2^+.[17] In ^{142}Sm this state will occur as a core excitation. Since this state involves mainly the protons (because of the neutron closed shell), it cannot be populated in a one-step (p,t)-reaction process. If the state we see in ^{142}Sm at 1659 keV is mainly this core excited state, that would explain both its small cross section and its anomalous angular distribution, since DWBA is by definition a theory of one-step processes.

The states at 2025 and 2747 keV contain 14.6% and 3.6% of the strength of the first excited state, respectively. Therefore we have observed the number of 2^+ states which are expected, provided there is no extensive mixing of the two-hole strength with core or proton excitations.

3. Other positive-parity states

One 4^+ and one probable 6^+ state, at 1791.3 and 2420.0 keV, respectively, have been observed in the beta decay of ^{142}Eu.[10] The lowest configuration contributing to (p,t) strength will be $(h_{11/2}^{-2})$. There is a relatively strong $L=4$ transition at 1790 keV and four other states, at 2418, 2582, 2867, and 2955 keV, whose angular distributions agree best with $L=4$. There are three core states observed in ^{144}Sm below 3 MeV which have spins and parities of 4^+.[17] Of course, one can generate states with a spin and parity of 4^+ by couplings such as $[(d_{3/2}^{-2})^{2+} \times \Psi_{\text{core}}{}^{2+}]^{4+}$. Weak mixing of the $(h_{11/2}^{-2})_{4+}$ with such states can account for $L=4$ strength in a number of states.

It is surprising that we do not see an identifiable 6^+ state. DWBA calculations predict that the $(h_{11/2}^{-2})_{6+}$ state should be easily seen in our experiment. However, we populate a state at 2418 keV whose energy agrees very closely with the 2420-keV state identified as a probable 6^+ state in ^{142}Eu beta decay. Our angular distribution (Fig. 2) does not agree with the DWBA $L=6$ prediction, but it is certainly possible that this is, in fact, a 6^+ state or that we are observing an unresolved doublet.

4. Negative-parity states

Six negative-parity states can be generated by the $(d_{3/2}^{-1}h_{11/2}^{-1})$ and $(s_{1/2}^{-1}h_{11/2}^{-1})$ configurations. Only three states with negative-parity have been

observed by beta decay.[10]

A 3^- state has been observed at 1784.1 keV. It undoubtedly corresponds to the 1810.1-keV octupole state seen in ^{144}Sm.[17] Since this is a particle-hole state it will be populated only weakly in the (p,t) reaction and we do not resolve it from the intense 4^+ state at 1790 keV.

The other two negative-parity states seen in beta decay are at 2347.9 and 2372.0 keV and are assigned as 5^- and 7^-, respectively. The 7^- state should be a nearly pure $(h_{11/2}^{-1}d_{3/2}^{-1})_{7^-}$ state while the 5^- can contain, in addition, a component of the $(h_{11/2}^{-1}s_{1/2}^{-1})_{5^-}$ configuration. The most intense state in our spectrum occurs at 2351 keV. It appears that we have not resolved the 5^- and 7^- state. Nevertheless, we have plotted the angular distribution for this peak in Fig. 8 together with the DWBA predictions. A combination of the 5^- and 7^- distributions in which the contributions are approximately equal at 45° gives a reasonable fit to the data except at forward angles. Levels with spins 5^- and 7^- have also been populated in the isotone ^{138}Ce by means of a (p,t) reaction with 20-MeV protons.[19] This case shows a similar discrepancy between DWBA theory and experiment at forward angles. It is probable that many of our uncharacterized levels can be attributed to states with negative parities since this is the major source of unassigned (p,t) strength.

B. *n*-particle, two-hole states in the even samarium isotopes

In Fig. 9(a) we present a simplified diagram for the shell structure of the ground state of ^{148}Sm. The valence neutrons are in the $2f_{7/2}$ orbital. In a (p,t) reaction leading to ^{146}Sm, the transferred neutrons can be removed from the valence orbitals, from levels below the $N=82$ core, or from both the valence orbitals and the core orbitals. Figure 4 clearly shows that in ^{146}Sm and ^{148}Sm there is a concentration of strength associated in energy with the discrete states seen in ^{142}Sm. This suggests that a significant fraction of the strength comes from removing two neutrons from the core. In addition, there are narrow structures, some of which are correlated in all the nuclides. We will discuss these features in the following subsections.

1. Gross structures in the (p,t) spectrum from Sm

Any strength associated with two holes in the $N=82$ core, i.e., with the low-energy states in ^{142}Sm, will occur at a relatively large excitation energy in the heavier isotopes. It should be possible to estimate this excitation energy from nuclear masses provided we possess enough information to calculate the diagonal interactions of the particles and the holes among themselves and with the ^{144}Sm core.

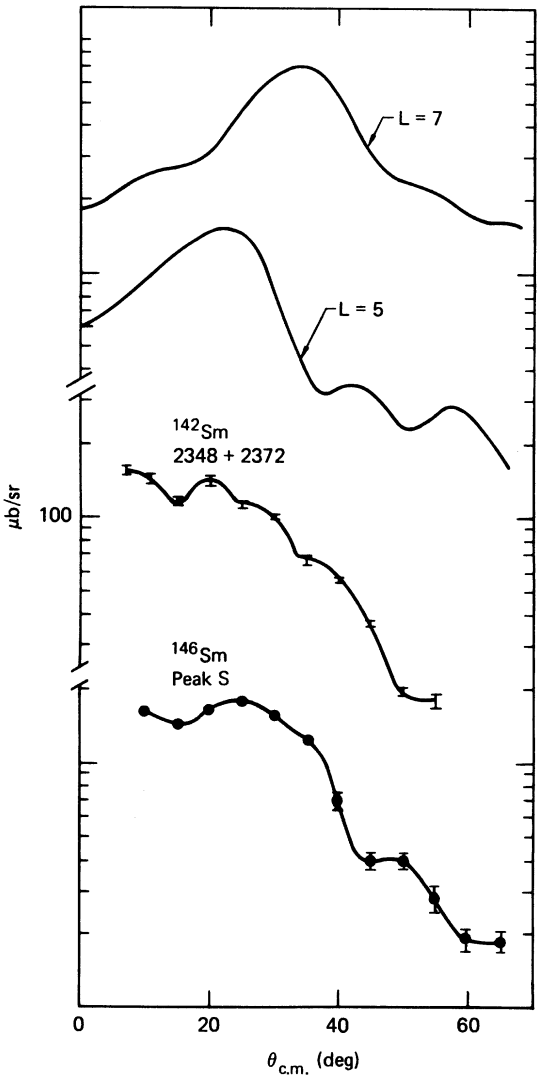

FIG. 8. Angular distributions of tritons from the (p,t) reaction associated with the (unresolved) levels at 2348 and 2372 keV in ^{142}Sm and with the peak *S* (see Fig. 7) in ^{146}Sm. The results of DWBA calculations for $L=5$ and $L=7$ are shown at the top. The lines through the data are only to guide the eye.

In Fig. 9(b), we show a pictorial representation of the excitation energy for a 4p-2h state in ^{146}Sm. If this represents the lowest 0^+ state from such a configuration and if we ignore configuration mixing and the effect of diagonal (p-h) interactions, then the excitation energy can be related to ground-state masses. The diagrams between the equality signs represent the excitation energy in the approximation where there is no configuration mix-

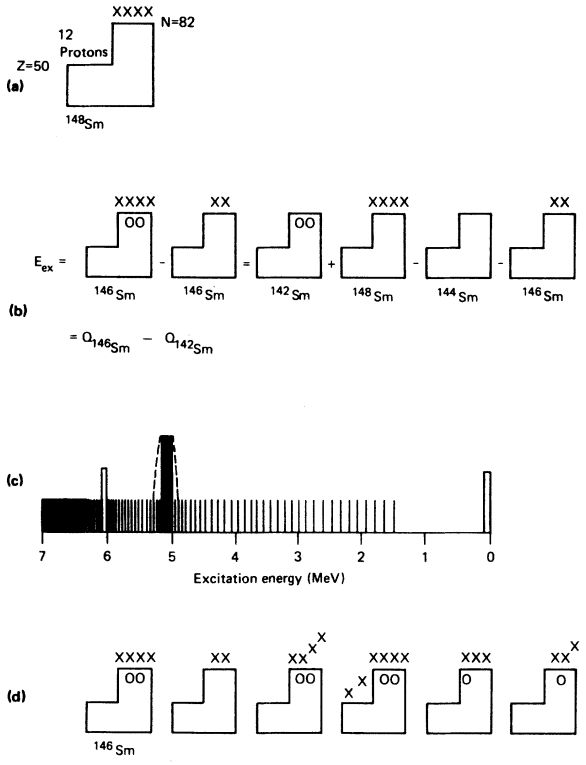

FIG. 9. Schematic shell-model representations. (a) The shell structure for ^{148}Sm. (b) A shell-model mass formula for estimating the excitation energy for the lowest four-particle two-hole O^+ state in ^{146}Sm. (c) A "picket fence" representation of the level density for ^{146}Sm in the noninteracting quasiparticle model. The dashed line represents weak damping of the two-hole state. (d) A two-hole state and the ground state for ^{146}Sm, followed by other excited configurations that can mix with the two-hole state. The fourth diagram represents a two quasiproton state built on the first diagram.

ing. The first three terms to the right of the second equal sign represent the mass of the 4p-2h state in the approximation where in addition to ignoring mixing we ignore the p-h interactions. The algebraic sum of the four masses, which is the excitation energy in this approximation, is rigorously the difference of the two Q values. The contribution from p-h interactions is difficult to obtain from experiment since it requires information on neutron p-h excited states in ^{144}Sm obtainable only with radioactive targets.

This result is in qualitative agreement with the evidence displayed in Fig. 4. There we have drawn dashed lines through the ^{148,150,152,154}Sm(p,t) data to guide the eye. Each line has the same slope and nearly the same intercept on the vertical axis. These parameters are established by the data at the highest excitation energies. At these energies we expect changes in the nuclear structure, and hence in the cross sections, to remain relatively unaffected by the addition of neutrons at the Fermi surface.

Relative to these reference lines, there is a broad bump in the (p,t) cross sections to ^{146}Sm and ^{148}Sm. The bump is centered roughly at the Q value of the low-lying states in ^{142}Sm. This region is denoted by the two right-most arrows in the second panel of Fig. 4. In the ^{152,154}Sm(p,t) data the association with strength in ^{142}Sm effectively disappears. The right edge of the bump vanishes because the cross section increases, while the strength under the bump is broadened.

Such behavior is consistent with a dramatic change in shell structure in which the $N=82$ gap disappears. This picture predicts a dissipation of the bump's strength as the orbitals associated with the ^{142}Sm valence nucleons fragment into several Nilsson states. In addition, there is a substantial increase in two-nucleon pickup strength at the low excitation edge of the bump, due to the addition of strength from the valence (i.e., $N>82$) neutrons. This strength is no longer isolated from the bump by a large shell gap.

The question of the strength of the resonance remains. How much of the strength in the bump comes from two-hole strength observed in the ^{144}Sm(p,t) reaction? There may be other contributions to the bump region due to (p,t) strength associated with states populated through higher-order reaction processes or to (p,t) strength from two-hole states where at least one of the holes is in a valence orbital. To investigate this question we integrated each spectrum between the Q values -8.8 and -16.5 MeV. The region of integration is shown by arrows in the second pannel of Fig. 4. We have presented the angular distributions for this region in Fig. 5. All nuclides have the same structureless, monotonically decreasing angular distribution. However, the integrated cross sections for ^{142}Sm are approximately a factor of two smaller. Thus, up to about 50% of the strength in the bumps could derive from the transfer of valence nucleons.

The angular distributions are structureless since many states with different spins and parities contribute to the strength in the region we are considering. A summation of the DWBA curves presented in Fig. 2 yields a qualitatively similar result.

The total strength in our integration window is ~15% larger for the deformed isotopes. One can understand this since the deformed targets have the greatest number of neutrons in the valence shells and so have a larger cross section for two-neutron pickup. As the $N=82$ shell gap disappears

with deformation, that strength can mix into the energy region associated with the bump.

We have also integrated a narrower region immediately above the excitation energy of the bump and plotted its angular distribution in Fig. 6. Figures 5 and 6 are qualitatively similar except that in the higher-energy distributions the slope is not as great and the difference in cross section between ^{142}Sm and the other isotopes is not as large. The slope is consistent with DWBA predictions for more negative Q values. Since we have attributed the difference in strength between ^{142}Sm and the other isotopes at least in part to the pickup of valence nucleons, we expect that at higher excitation energies the cross sections will approach each other since the fraction of states associated with removal of valence nucleons decreases with excitation energy.

2. *Narrow structures at large excitation energy*

At approximately 5 MeV of excitation energy a narrow peaklike structure (c) is observed in ^{146}Sm (see Fig. 4). This was quite unexpected since the level densities at these excitation energies should be large for heavy nuclei. Thus, unless there is some unique symmetry, we expect the residual interaction to severely fractionate the strength of individual peaks. In Table IV we present estimates of the nuclear-level densities for ^{146}Sm and ^{148}Sm as a function of spin and parity. These were calculated using the Gilbert-Cameron level-density formalism with Cook-modified parameters.[15]

High-resolution experiments with the QDDD spectrograph and the thin ^{148}Sm target were discussed in the previous section and displayed in Fig. 7. The region between A and B in this figure corresponds to peak c in Fig. 4. We have analyzed this portion of the spectrum using the peak analysis code AUTOFIT.[20] The result of the fit for 25° is also displayed in Fig. 7. The peaks are superposed over a continuum which is approximated by the dashed line.

TABLE IV. Predicted level densities in ^{146}Sm and ^{148}Sm.

Angular momentum	Level density (No./keV) ^{146}Sm	^{148}Sm
0	0.03	0.3
1	0.08	0.7
2	0.13	1.2
3	0.16	1.5
4	0.18	1.7
5	0.18	1.8
6	0.17	1.7
7	0.15	1.6
8	0.13	1.4
9	0.10	1.2
10	0.08	1.0

We have identified 12 peaks, a number far less than expected from the calculated level densities. Thus, we assume that not all the peaks have been resolved. This is consistent with our observation that none of the peaks that we analyzed in Fig. 7 have a readily recognizable angular distribution although they definitely show structure. The underlying continuum can be attributed to unresolved peaks.

Although we have performed high-resolution experiments only for the region centered at 4.87 MeV in ^{148}Sm, the following explanation for peaks a, b, and c in Fig. 4 seems quite plausible.

Oelert *et al.*[12] searched for 0^+ and 2^+ pair-removal vibrational strength in the Sm isotopes in a (p,t) experiment by using 25-MeV protons. They did not find any strength even though 2^+ pair removal states were populated (but using much higher proton energies) in the Nd isotopes. They concluded that such states did not appear in their Sm experiments because of a strong dependence on the proton beam energy for their population. However, they used systematics to predict the position of these states in the even Sm isotopes. Peak a corresponds almost exactly to their prediction for the position of the 2^+ pair removal states. The relative energies and strengths of peaks a, b, and c are qualitatively the same in ^{146}Sm and ^{142}Sm, suggesting that they have similar origins. Furthermore, some support for such a correlation between peaks a, b, and c in the two nuclides comes from the angular distribution of the doublet labeled S in Fig. 7. This angular distribution is similar to that of the $(5^-, 7^-)$ doublet labeled c in the ^{142}Sm spectrum of Fig. 4 (the 2351-keV peak in Fig. 1) and is consistent with our DWBA prediction for the $(h_{11/2}^{-1}d_{3/2}^{-1})$ mixture of a 5^- and 7^- state. (See previous discussion in Sec. IV A 4.) This is illustrated in Fig. 8 where the relevant experimental and theoretical angular distributions are plotted. Unfortunately, we did not measure absolute cross sections in the QDDD experiments at Princeton. However, we can compare cross sections by integrating the MSU data for peak c over the same solid angle for which the ^{142}Sm cross sections that are listed in Table II were determined. This integration gives for peak c in the ^{148}Sm$(p,t)^{146}$Sm reaction a cross section of 74 μb for the solid angle contained between 5° and 58° from the beam axis. By comparison with the value of 172 μb from Table II for the peak at 2351 keV (the 2348- and 2372-keV doublet), we see that the strength of the ^{142}Sm states is sub-

stantially fragmented in ^{146}Sm.

The strength of peak c decreases rapidly as a function of mass (see Fig. 4). This can be explained because the 5^- and 7^- states in ^{142}Sm are predominantly $(h_{11/2}^{-1}d_{3/2}^{-1})$. With increasing deformation both the $h_{11/2}$ and $d_{3/2}$ strength fragments into several Nilsson orbits with different energies. Thus, the negative-parity strength is strongly fragmented with deformation. Moreover, the level density of all spins and parities is much higher in ^{148}Sm than in ^{146}Sm. Nevertheless, some strength appears to remain at the same Q value as in ^{146}Sm.

An important question is why the damping of the 2^+, 4^+, and 7^- two-hole structures (peaks a, b, and c) is so weak. This can be explained in terms of the density and the structure of states occurring in the same energy region as the two-hole states.

Figure 9(c) is a schematic representation of the density of levels with a given spin and parity in ^{146}Sm. A two-hole state (such as peak a in Fig. 4), closely related to a low-energy state in ^{142}Sm, is represented by the black bar. Complex multiple-quasiparticle states are indicated by thin black lines. The open bars represent states that can be connected to the black bar by a single two-nucleon scattering, i.e., mixed in first-order perturbation theory.

Figure 9(d) illustrates the structure of a select set of configurations in ^{146}Sm, each with the same spin and parity. The first diagram represents the weakly damped two-hole state. The other diagrams are the ground state, followed by excited configurations which can mix with the two-hole state. All these excited configurations except the last one are clearly separated from the two-hole state by at least a pairing gap. States represented by the last diagram may have energies similar to the two-hole state, but the level density of such states is much too low to produce significant damping of the two-hole state. Therefore, the damping for states other than 0^+ should be relatively weak since it occurs only through small admixtures in the wave function of the two-hole structure. The 0^+ states are unique since they can mix with the ground state through a particularly large matrix element of the residual interaction.

A detailed explanation for the peaks labeled e is not possible from our experiments. Nevertheless, it appears likely that they will be associated with two-hole strength in the steeply upsloping Nilsson orbitals originating below the $N=82$ shell. Recent experimental results[21] show that at least in ^{152}Sm peak e is similar to peak c in ^{146}Sm, i.e., a large narrow peak with a cluster of weaker peaks in its vicinity.

There appears to be significant narrow structure with the ^{152}Sm and ^{154}Sm targets in the region of $Q=-17$ to -18 MeV. Since these structures presumably involve the removal of two nucleons from far below the Fermi surface, and since the targets are strongly deformed, they may give experimental evidence that deformed nuclei maintain a spherical core.

V. SUMMARY AND CONCLUSIONS

We have performed a series of (p,t) experiments on the stable Sm isotopes. Most of the experiments were performed at MSU where we obtained low-resolution data to ~15 MeV in excitation energy. Somewhat better resolution was obtained for the levels in ^{142}Sm. A high-resolution experiment was performed with a QDDD spectrometer at Princeton University for a 1.5-MeV region near 5 MeV in excitation energy for ^{146}Sm.

We have analyzed the ^{142}Sm data and have identified a number of peaks previously seen only in the decay of ^{142}Eu. We have identified a number of other 0^+, 2^+, and 4^+ states and characterized them with respect to likely shell model configurations. We have also observed a number of new, but as yet uncharacterized, levels.

The low-resolution experiments show a concentration of (p,t) strength in ^{146}Sm and ^{148}Sm for two holes below the $N=82$ shell gap. This disappears or at least is substantially broadened for ^{150}Sm and ^{152}Sm. This happens because the shell structure associated with ^{142}Sm is destroyed with the onset of deformation between $N=88$ and 90. The total strength in the region of the bumps is nearly twice that seen in the comparable-Q window for ^{142}Sm. This implies that much of the strength occurs by removal of one or more valence nucleons and/or through higher-order processes.

A number of reproducible narrow structures remain at excitations in excess of 4 MeV. Some of these can be correlated with individual peaks in ^{142}Sm and can be explained by the existence of pairing gaps. Some weakly populated but clearly observable structures occur at nearly the same Q value in ^{150}Sm and ^{152}Sm. They presumably involve removal of nucleons from orbitals far below the Fermi surface, where the distribution of matter and hence the self-consistent nuclear field are unaffected by changes in the nuclear shape.

There are a number of experiments which may answer remaining questions. A ^{146}Sm(p,t) experiment would identify the pairing vibrational states and perhaps give a clue to the fate of the missing 0^+ strength. All the narrow structures should be examined with improved resolution. This is also

true for the entire ^{142}Sm spectrum. A ^{147}Sm(p,d) experiment would identify strength associated with one valence particle in the region of interest and, of course, a ^{145}Sm(p,d) experiment would permit an estimate of the neutron p-h interactions necessary for an accurate theoretical prediction of the resonance energies in the weak-coupling model. Unfortunately, the experiments with ^{145}Sm and ^{146}Sm require fabrication of radioactive targets that will be difficult to obtain. Finally, similar experiments on the Nd and Ce isotopes would yield valuable additional systematic information.

ACKNOWLEDGMENTS

This work was performed in part under the auspices of the U. S. Department of Energy by the Lawrence Livermore Laboratory under Contract No. W-7405-ENG-48 and under the auspices of the U. S. National Science Foundation under Grant No. PHY78-22696.

---

*Permanent address: Institut de Physique Nucleaire, B.P. No. 1, 91406 Orsay, France.

[1]A. Bohr and B. Mottelson, *Nuclear Structure* (Benjamin, New York, 1975).
[2]D. J. Horen, F. E. Bertrand, and M. B. Lewis, Phys. Rev. C 9, 1607 (1974).
[3]R. A. Broglia and D. R. Bes, Phys. Lett. 69B, 129 (1977).
[4]G. M. Crawley, W. Benenson, D. Weber, and B. Zwieglinski, Phys. Rev. Lett. 39, 1451 (1977).
[5]G. L. Struble, L. G. Mann, R. G. Lanier, W. M. Buckley, J. Kern, G. Crawley, S. Gales, D. Mueller, and F. Girshick, Phys. Lett. 93B, 26 (1980).
[6]R. Kouzes and W. H. Moore, Phys. Rev. C 12, 1511 (1975).
[7]R. G. Markham and R. G. H. Robertson, Nucl. Instrum. Methods 129, 131 (1975).
[8]A. H. Wapstra and K. Bos, At. Data Nucl. Data Tables 19, 215 (1977).
[9]W. Stöffl, Tech. Univ. of Munich, Garching, Germany, computer code FITEK (private communication).
[10]G. G. Kennedy, S. C. Gujrathi, and S. K. Mark, Phys. Rev. C 12, 553 (1975).
[11]D. Habs, H. Klewe-Nebenius, R. Löhken, S. Göring, J. van Klinken, H. Rebel, and G. Schatz, Z. Phys. 250, 179 (1972).
[12]W. Oelert, G. Lundstrom, and V. Riech, Nucl. Phys. A233, 237 (1974).
[13]P. D. Kunz, University of Colorado, Boulder, Colorado, computer code DWUCK (private communication).
[14]C. M. Perey and F. G. Perey, At. Data Nucl. Data Tables 17, 1 (1976).
[15]A. Gilbert and A. G. W. Cameron, Can. J. Phys. 43, 1446 (1965); J. L. Cook, H. Ferguson, and A. R. Musgrove, Australian Atomic Energy Commission Report No. AAEC/TM392 (1967).
[16]R. G. Lanier, G. L. Struble, L. G. Mann, I. D. Proctor, and D. W. Heikkinen, Phys. Rev. C 18, 1609 (1978).
[17]*Table of Isotopes* edited by C. M. Lederer and V. S. Shirley (Wiley, New York, 1978).
[18]R. K. Jolly and E. Kashy, Phys. Rev. C 4, 887 (1971).
[19]J. D. Sherman, D. L. Hendrie, and M. S. Zisman, Phys. Rev. C 15, 903 (1977).
[20]J. R. Comfort, ANL Report No. PHY-1970B (unpublished).
[21]A. Saha, O. Schotlen, D. C. J. M. Hageman, and H. T. Fortune, Phys. Lett. 85B, 215 (1979).